University of Thi -Qar Journal for Engineering Sciences
http://www.doi.org/10.31663/tqujes.12.2.443(2022)
Vol 12.2(December 2022)

ISSN :2664- 5572 (online)
ISSN:2664-5564 (print)
Available at http://jeng.utq.edu.iq
utjeng@ utq.edu.iq

Numerical simulation of ash deposition on the surface of tubes bundle

Elaf A. Hasson[†], Adnan A. Ateeq[‡] and Tahssen A. Jabbar[ł]
Elafali091@gmail. com[1+,] adnan_ateeq@stu. edu. iq [‡,] tahseen. ali@stu. edu. iq[†]
Department of Thermal mechanical Engineering , college of Technical Engineering.Southern Technical University

Abstract
Ash deposition is one of the significant challenges for coal-fired boilers. It is a serious problem that causes fouling and slagging on the tube bundle that Poses some potential safety and hazard problems for utility boilers. There. Therefore, the paper presented a numerical study using ANSYS FLUENT. A discrete phase model (DPM) is used to simulate ash particles for unsteady flow. The influence factors important to heat transfer performance and ash deposition are studied, consisting of the changes of the inlet velocity of flue gas, and the temperature differences between the flue gas and the surface of ash deposit. A thermophoresis deposition mechanism (fine particles< 1µm) is a playing impact in an important role in this study. The proposed method is an effective instrument for forecasting the ash deposition formation and growth. The result indicates thermophoresis causes more ash to be deposited than without thermophoresis. Also, they notice the effects of temperature gradient on the deposition height at constant inlet velocity. The deposition height is decreased when the temperature differences increase as a ratio of 0.125%. through 30 min. While the effects change inlet flue gas velocity on the deposition height. The deposition height is decreased when the increased velocity at constant temperature differences about 0.75%.

Keywords: Ash deposition, CFD Modeling, DPM.

1. Introduction

A deposit of ash on the heat transfer surface of heat exchangers. It has led to several operational issues (slagging and fouling, corrosion, and erosion) that cause safety problems and some potential hazards to utility boilers**[1].**
resulting in economic losses and safety risks **[2]**.Result presence of mineral mater in the fuel. A mineral substance has undergone physical and chemical processes producing particles of ash deposition volatile gases which mix with the flue gas. The minerals present in coal can lead to serious operational problems in boilers **[3][4]**. Therefore, it is very important to better understand the formation process of ash deposits in order to minimize these problems. In addition, it can be used to optimize the design and operation of the boiler. On the basis of previous experimental and theoretical studies**[5][6].** The ash deposition can be affected by several factors, such as fuel quality, operation conditions, and the arrangement of heat exchangers **[7].** In spite, the boiler design has been changed and routine soot blowing systems have been employed to minimize the detrimental effects of fouling and slagging. There are still uncontrolled and unexpected problems where the cleaning system cannot reach the deposit or the bonding strength between the deposits and the wall is too strong for the cleaning system to work [8]. Therefore, It's important to use numerical modeling to predict the deposition of ash. In CFD, there are generally two simulation approaches, one is a steady state, and the other is a transient or non-steady state. Modeling steady states using the steady state approach is common in the behavior of ash deposition in combustion systems**[9][10]**. By tracking a fixed number of particles and simplifying the deposition process without considering the growth of ash deposits, this approach can save computing time. As opposed to the transient approach, which considers the change of some parameters with time (e.g. deposition rate, surface temperature, and ash deposit shape), the transient approach is usually used to simulate ash deposit growth**[11][12]**. As a matter of fact, ash deposition on the tubes in boilers is a dynamic process for many parameters to change during the ash deposition process. As a result, the transient approach is considered more appropriate to simulate the growth of ash deposits, which is also intended to have a greater accuracy compared to steady state simulations. Several studies were done on how fly ash deposition affects heat exchanger tube bundles to improve heat transfer efficiency and reduce ash-related problems. There are several researches focused on the deposition mechanisms and the behavior of the deposition during combustions have been studied extensively. Ash deposition mechanisms are studied by many authors. Inertial impactions, eddy impaction, thermophoresis, condensations, chemical reactions, pressure gradient and virtual forces are of the process that control ash deposition. A heat-exchange tube's surface is affected by two factors that determine whether the impacting ash particles stick or rebound **[9].** Firstly, an analysis of particle properties such as particle temperature, chemical composition, impact velocity and angle, and particle size.
A second factor is affected by the surface properties of the ash deposits, such as their temperature, roughness, and stickiness. The surface temperature of an ash deposit is found to have a significant influence on its deposition [13][14][15]. A high temperature on the surface of an ash deposit can increase the stickiness of the surface, thereby increasing the probability of capturing ash **particles [16].** In spite of this fine particles (<10µm) can also be reduced

due to the decreased temperature gradient between the flue gas and the surface of the ash deposits[17].

S. Balakrishnan a, **[18]** studied the mechanisms thermophoresis, forces. R. Weber, et [19], it is performed inertia impaction, through use CFD code, we have shown that accurate impaction efficiency predication is only possible if the flow field around the deposition surface is well resolved. H. Zhou **[20]**, this studied sub models of deposition are included in the model (condensations, Brownian and eddy diffusions). But Yang et al. **[12]** the result show as deposition under high furnace temperatures is dictated by particle deposition resulting from inertia impaction. And It was found that condensation had a less significant influence on deposition compared to the other mechanisms'. Zhou **[21]** studied the saffman forces, pressure gradient and virtual forces. The above review the mechanisms ash deposition. In few simulations, ash deposition on the tube bundles has been examined in relation to deposit surface conditions. Therefore, this current study aims to develop computational fluid dynamics by using ANALYSIS FLUENT R12020 tools through using (DPM) discrete phase model to predict the simulation ash deposition of tube bundles and the mechanisms thermophoresis with different temperature between the surfaces wall temperature and inlet flue gas. The mechanisms thermophoresis was considered for ash depositions. They noticed in this study, the results show that the accumulative ash depositions in the four row increase with time and the front row the accumulative deposition is higher than of the two rows last

2. Model description and numerical method

2.1 physical model

As shown fig (1) the schematic diagram of Two-dimensional domined model with four- rows is simulated deposition on the tube bundle in boiler. The computational domain is given of the four-rows tube, the value of tube diameter (D= 38mm), the transverse pitch(St =100mm), and the longitude pitch (Sl=100mm).The length and width of the domain are 800 mm and 400 mm. Commercial CFD fluent is used frame work to solve the turbulent fluid flow, gas and the particle combustion. The tube bundle in the boiler was simulated to be operating with upstream gas velocity 0.407 m/s, tube wall temperature of Tw=600 Kand a gas flow temperature of Tin=1500 K . The simulation implement was deposition model through Discrete phase model (DPM) was chosen, the flue gas containing five components is respecting (vol%), O2= 4.7, H2O = 10.0, CO2=13.6. N2=80.7.

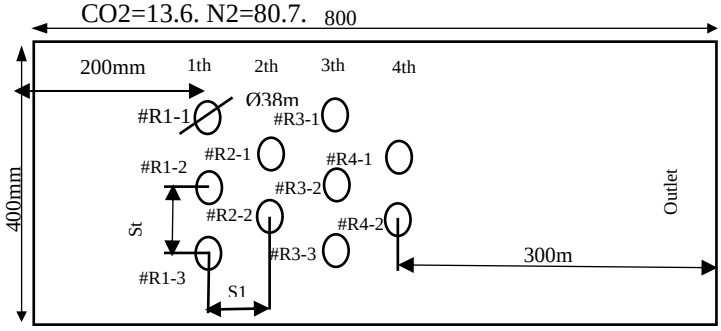

Fig.1 The geometry of tube bundle arrangement with four rows

2.2 Numerical solution and boundary conditions.

The numerical simulation (CFD)in unsteady was performed by using ANYSIS FLUENT R1-2020. The gas flow is simulated in turbulent model is accounted with realized k-ε model with enhanced wall treatment. A pressure- velocity coupling with the SIMPLE algorithm. The second order upwind discretization. The governing equation is used in turbulent fluid including (continuity, momentum and energy equation are solved for the continuous gas phase flow). Fig 2 illustrates, the number of the node on the deposition tube is 200 elements. The time step size of 0.009 s with seventy max Iterations. Discrete phase model (DPM) was chosen, the particles are injected through the inlet surface with the same the inlet velocity of flue gas and the diameter distribution using (rosin-rammler) of particle (min. diameter1µm, mean. diameter 16 µm, max. diameter 62. The boundary condition of flue gas and ash are showed in tables 1 and2.

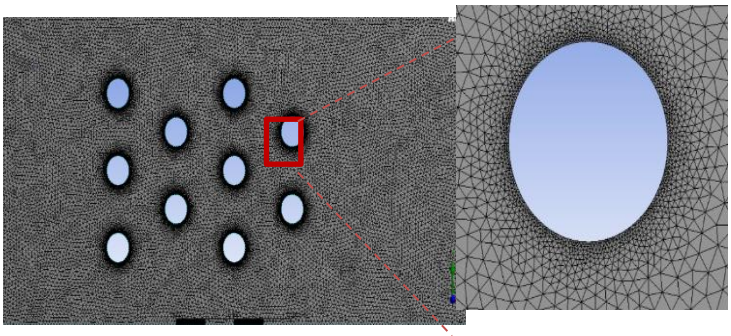

(a)all domain (b)on pipe

Fig .2 The grid of computational domain

Table 1 Flow gas boundary condition:

Item	Value
Inlet temperature of flue gas(K)	1500
Inlet velocity of flue gas (m/s)	0.407
Inlet velocity of ash particle (m/s)	0.407
Wall temperature of furnace (K)	1500
Inlet temperature of ash particle	1500
Inlet wall temperature of the tube (K)	600

Table 2 Property parameters of ash deposition

Items	Value
Max diameter (μm)	60
Min. diameter(μm)	1
Average diameter (μm)	16
Density(kg/m^3)	1500
Specific heat capacity (J/kg. K)	1680
Thermal conductivity (W/m. K)	0.33
Flow rate of particle (kg/s)	0.001
Spread parameter	3.5

2.3 Governing equation:

The governing equations are applied to operate the mathematical model (Naiver- Stokes and energy equations for the computational domain's flue gas phase [22]. The simulation flow is 2D and unsteady.

The continuity equation is:

$$\frac{\partial \overline{\rho u_i}}{\partial x_i}=0 \qquad (1)$$

The Momentum equation:

$$\frac{\partial \overline{u_i}}{\partial t}+u_j\frac{\partial u_i}{\partial x_j}=-\frac{1}{\rho}\frac{\partial p}{\partial x_i}+\mu\frac{\partial^2 \overline{u_i}}{\partial x_i \partial x_j}-\frac{\partial}{\partial x_j}u'_i u'_j \qquad (2)$$

The Energy equation:

$$\frac{\partial T}{\partial t}+\frac{\partial}{\partial x_i}(u_i T)=\frac{\partial}{\partial x_i}\left(\frac{\lambda}{\rho cp}\frac{\partial T}{\partial x_i}\right) \qquad (3)$$

Where $\overline{u_i}$ and $\overline{p}$ are the time -averaged velocity and pressure, respectively. μ is the gas dynamic viscosity, ρ is the density of gas, T is the Temperature, c_p is the specific heat capacity. λ is the thermal conductivity.

The modeled transport equations for k and ε in the realizable k- ε model [23].

$$\frac{\partial}{\partial t}(\rho k)+\frac{\partial}{\partial x_j}(\rho k u_j)=\frac{\partial}{\partial x_j}\left[\left(\mu+\frac{\mu_t}{\sigma_\varepsilon}\right)\frac{\partial k}{\partial x_j}\right]+G_k+G_b-\rho\varepsilon-Y_m+S_k \qquad (4)$$

And the turbulent dissipation rate equation (ε) can be given by:

$$\frac{\partial(\rho\varepsilon)}{\partial t}+\frac{\partial}{\partial x_j}(\rho\varepsilon u_j)=\frac{\partial}{\partial x_j}\left[\left(\mu+\frac{\mu_t}{\sigma_\varepsilon}\right)\frac{\partial \varepsilon}{\partial x_j}\right]+\rho C_1 S-\rho C_2\frac{\varepsilon^2}{k+\sqrt{\nu\varepsilon}}+C_{1\varepsilon}\frac{\varepsilon}{k}+C_{3\varepsilon}G_b+S_\varepsilon \qquad (5)$$

Where $C_{3\varepsilon}=\tanh\left|\frac{v}{u}\right|$ and $C_{1=max}\left[0.43,\frac{\eta}{\eta+5}\right]$

$\eta=S\frac{k}{\varepsilon}$ S=$\sqrt{2S_{ij}S_{ij}}$

Table 3empirical constant for k-ε

C_μ	$C_{1\varepsilon}$	σ_k	σ_ε	C_1	C_2
0.09	1.44	1.00	1.3	1.8	0.6

2.4 DPM model

The particle motion, the trajectory of a discrete particle model (DPM), in this study to predict behaviours of particle ash deposition. The force acting on the particle by using governing equations of the parcel be written [24] .

$$F_i=\frac{18\mu}{\rho_P d_P^2}\frac{CD}{24}(u_i-u_{Pi})+g_i\left(1-\frac{\rho}{\rho_P}\right)+F_{gi}\ldots \qquad (6)$$

Where u_{pi} and u_i are the velocity of particle and gas, respectively (m/s); ρ is the density of gas (kg/m^3); μ is the molecular viscosity of gas(kg/m .s); D_P is the particle diameter (m); ρ_P is the density of particle (kg/m^3); Re is the particle Reynold number, the CD is the drag coefficient; g_i is the gravitational acceleration in I-direction(m/s^2) and $F_{gi}$is the additional force exerted on particles (m/ s^2)). The FD (the drag force) is the most important force in the forces analysis particle determined by [25].

$$F_D=\frac{18\mu C_d\, Re_P}{\rho_P d_P^2 24}\ldots. \qquad (7)$$

And Re is defined by

$$Re_P=\frac{\rho d_P|u_i-u_i^p|}{\mu}\ldots. \qquad (8)$$

Where Re_P is the particle Reynold number, the is the C_d drag coefficient, μ presents the viscosity of the gas phase and is d_P the particle diameter.The governing equation of particle motion [26] in this paper is given as follows:

$$\frac{du_P}{dt}=\Sigma Fi \ldots\ldots\ldots \qquad (9)$$

where the ΣFi represents various forces acting on the particle include. (thermophoresis, the drag, gravity, buoyancy, pressure gradient, Brownian, Saffman lift forces) influenced the mechanism of ash deposition. Both the Saff-man lift forces and the Brownian forces are important [27].The force balance of particle in flow field [21] : is described as

$$\frac{du_P}{dt}=\frac{18\mu C_d\, Re_P}{\rho_P d_P^2 24}.(u-u_p)+g\frac{g(\rho_P-\rho)}{\rho_P}\,\mathrm{F}\ \ldots\ldots\ldots(10)$$

Where, , $u_P, \rho_P, , d_P$ are the velocity ,density and diameter of particles, respectively; u, ρ represent the velocity and density of the gas phase c_D : denotes the drag coefficients, and F means other forces available in fluent such as(the thermophoresis forces, Saffman's lift forces, the virtual forces and pressure gradient forces), therefore perhaps simplified:

Thermophoresis forces .

Where the thermophoresis force F_T is represented [28] as:

$$F_T=-D_{T,P}\frac{1}{m_p T}\frac{dT}{dx} \qquad (11)$$

Where$D_{T,P}$ is the thermophoretic coefficient, you can define the coefficient to be constant [23]:

$$D_{T,p}=\frac{6\pi d_p \mu^2 C_s(K+C_t Kn)}{\rho(1+3C_m Kn)(1+2K+2C_t Kn)} \qquad (12)$$

Kn =Knudsen number =2λ/d_p

λ = mean free path of the fluid

k= fluid thermal conductivity based on translational energy only = (15/4) µR
$k_p = particle\ thermal\ conductivity$, $C_s = 1.17$, $C_t = 2.18$, $C_m = 1.14$
T= local fluid temperature
µ= fluid viscosity

The Brownian forces F_B is represent [23] as :

$$F_B = m_p \zeta_i \sqrt{\frac{\pi S_\circ}{\Delta t}} \quad (13)$$

Where $S_\circ$ is a Gaussian white noise random function , which is given by [29]

$$S_\circ = \frac{216\ \nu\ k_B\ T}{\pi^2 \rho\ d_p^5 \left(\frac{\rho_p}{\rho}\right)^2 C_c} \quad (14)$$

Where T is the absolute temperature of the fluid , v is the kinematic viscosity , C_c *is the* cunning correction , and k_B is the Boltzmann constant .

The Saffman's lift force F_S is driven in [30]

$$F_S = \frac{2\rho k \nu^{0.5} S_{ij}}{\rho_P (S_{ij} - S_{ij})^{1/4}} \quad (15)$$

2.5- Mesh in dependence

A mesh dependency test is generally performed to ensure that the result for CFD model is conducted for the case numerical simulation for ash deposition on the tube bundle. Fig (3) shows deposition height depends mainly on number of element. It is noticed the number of elements is a few form range (50-150) the result a great contrast of deposition height. While, the number of element is approximately constant form range (150-300) the result almost constant of deposition height. Future refinement is made number of element on the tube bundle

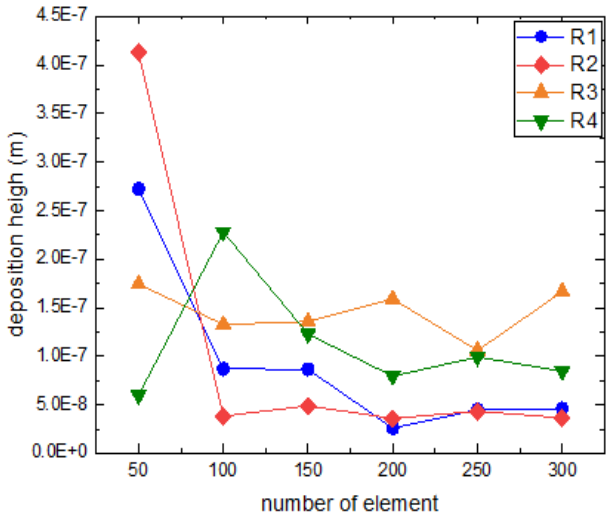

on 200 to achieve higher accuracy of measuring deposition

Figure. 3 Mesh independent.

3- Result and discussion

3.1 validation

To check the validity of the present study, verification must be done to compare with results of other researchers. Figure (4) illustrates a comparison of the numerical solution fig obtained and the results obtained from reference cite [21] for the same conditions. A 2D model is generated by using ANSYS fluent Design Modeler. The result of the present study is compared with the numerical and experimental result of the research S. Kalisz [31]. The fig (4) shows the accumulative deposits height on the pipe for a certain period of time. Since the time period used in this study and one presented by S. Kalisz [31], it was necessary to make the comparison in a non-dimensional way. Where H represent the ratio of accumulative deposition height at any time to accumulative deposition height at the end time of study. And X represent the ratio of the time to the total time of study. The simulation result logically converges with results obtained from reference cite [31].

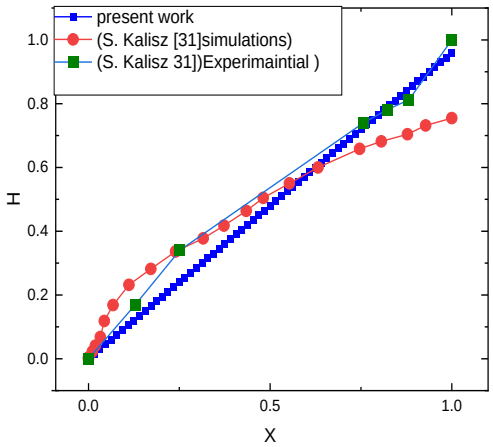

Fig. 4 validation at cite reference [31]

3.2 Effect of thermophoresis forces on ash deposit

3.2.1 Temperature contour of ash particle

Figure (5, a, b), shows DPM (ash temperature) temperature magnitude distributions in two cases through ten seconds and other five minutes. We observed a drop in the average temperature surrounding the tubes, which resulted in a low deposition mass. The result noticed in two cases the deposition for all rows increased with time. And It is found flue gas upstream has obviously higher temperature distributions. This tube's back has been protected by the front tubes, when viewed from the structure of the bundled tube resulting in low deposition mass, in the back rows

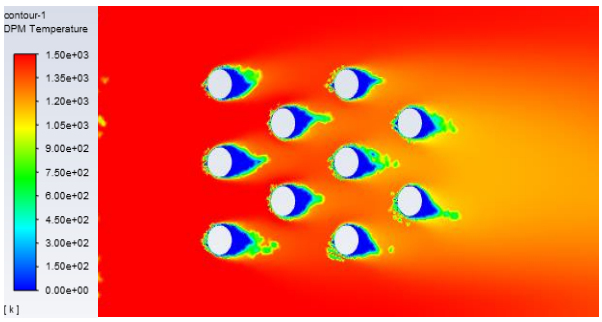

(a)t=10s

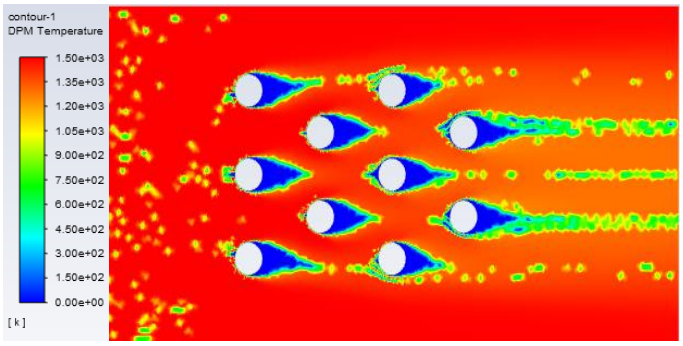

(a)

(b) t=5min

Fig.5 Temperature magnitude distribution

3.2.2 Effect the temperature difference

The temperature difference between the surface of tube and flue gas**(ΔT)** is changed from 0 to 1000 C° with step 100°C. The effect of the thermophoresis force on the accumulative deposition height is obvious than that without thermophoresis. The simulation result show that the temperature difference has a significant influenced on accumulative ash deposition. As shown, in fig(6-a), there is obvious higher accumulative deposition height at the temperature difference on (800C°) with thermophoresis for the first row on the tube (R1). The lowest the accumulative deposition height occurs at the temperature difference is (200C°). In fig (6-b) illustrates, there is obvious higher accumulative ash deposition height at the temperature difference on (900C°) with thermophoresis for second row on the tube (R2). The lowest the accumulative deposition high can see at temperature difference on (500C°) without thermophoresis. As shown in fig (6-c, d), there is obvious higher accumulative ash deposition height on the temperature difference (1000C°) with thermophoresis for third row and for four- row on the tubes (R3) (R4). The lowest the accumulative deposition high is found on (200C°) with out thermophoresis for(R3) and (600C°) without thermophoresis for (R4). They notice the effect thermophoresis forces increasing the accumulative deposition high than without thermophoresis

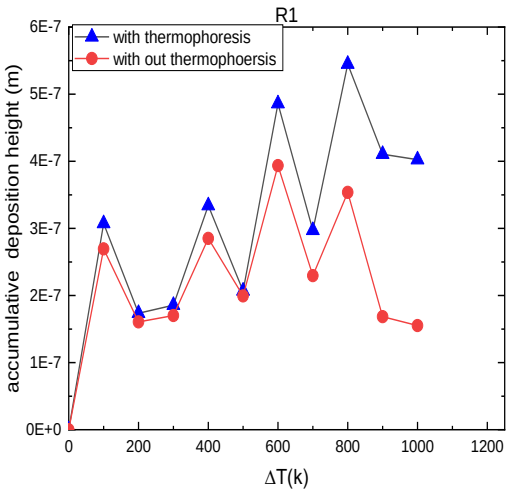

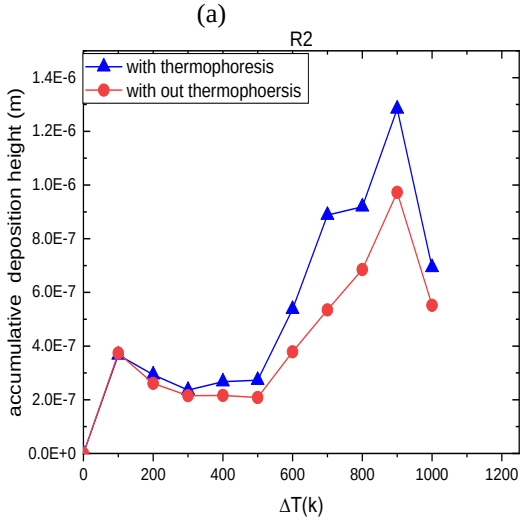

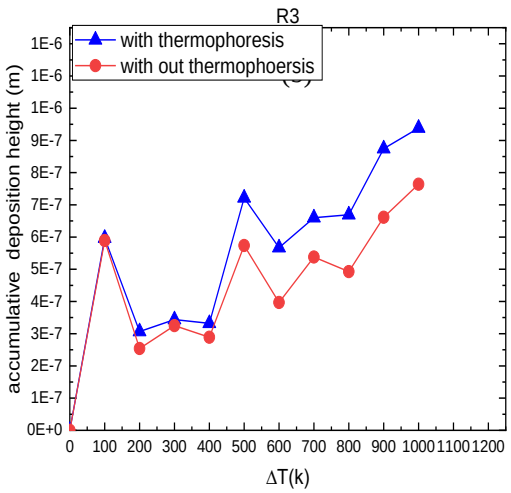

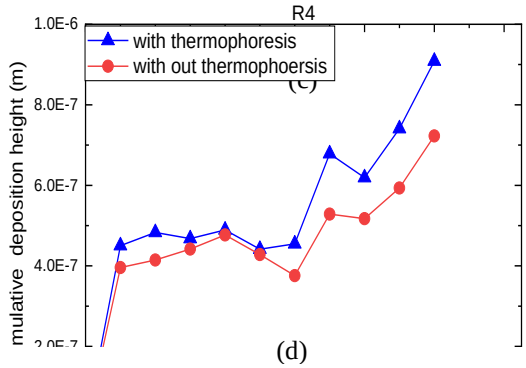

(d)

Fig. 6 The effect temperature difference on

3.2.3Effects of temperature gradient on the deposition height

As shown in fig (7) change velocity of flue gas about range form (0.1-0.2 m/s) has not significant influenced on the accumulative deposition height with thermophoresis and without thermophoresis. In fig (7-a and c), illustrates, the higher accumulative deposition height of the velocity flue gas on (0.9m/s) with thermophoresis for first raw and third row of tube. While the lowest the accumulative deposition height the velocity flue gas on (0.4 m/s) for first raw and (0.1m/s) for third row without thermophoresis. As it can be seen in fig(7-b) the higher deposition height on (0.8 m/s) with thermophoresis. while the lowest accumulative deposition height on (0.7 m/s) without thermophoresis for second row. In fig (7-d) the higher accumulative deposition height on (0.6-0.7 m/s) with thermophoresis for four row. while the lowest accumulative deposition height on the (1m/s) without thermophoresis. Because thermophoresis forces dependent on the velocity, temperatures and particles size very small. The stagnation point on the wind wared side of the first row tube, therefore the flue gas velocity inlet is relative low and then increases maximum value on the 1m/s. The main reasons of vortices have a significant influenced motion.

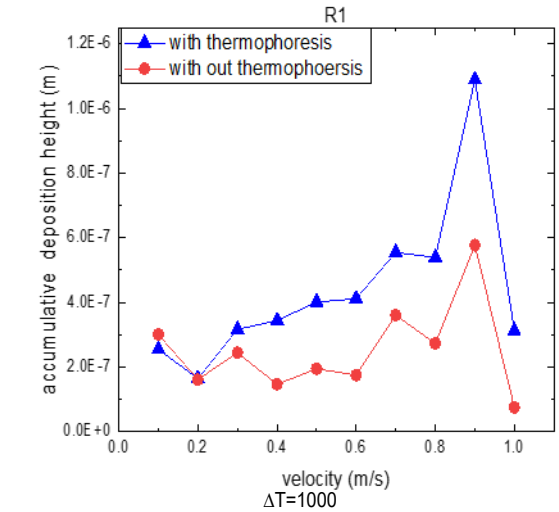

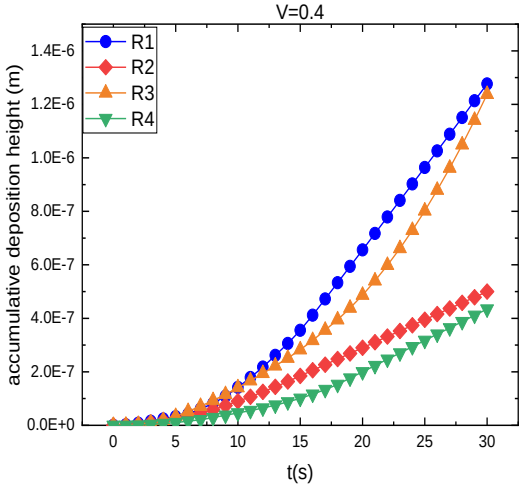

(c)

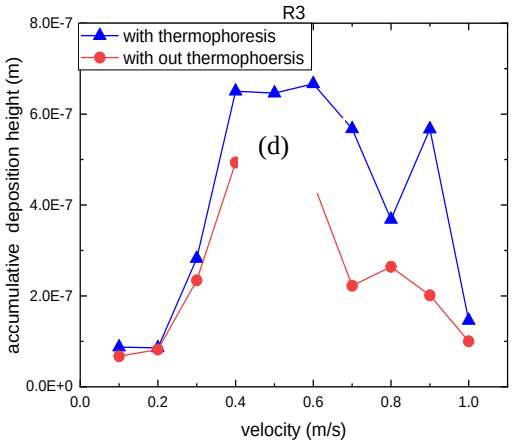

Fig.7 The effect velocity on the accumulative deposition height

3.3 Effects of temperature gradient on the deposition height

The temperature difference between the surface of tube and flue gas (ΔT). We will study the effect of temperature and flue gas on the deposition that get on the pipes through 30 second. Fig. (8), shows the deposition height of four rows of tubes. The results show that deposition height for all increases with time. Comparing the constant velocity and varying temperature difference between the inlet flue gas and the surface tube with thermophoresis forces. Fig (8-a), (8-b), it can be seen the first row of the tube has a higher deposition. Since it is shielded by the front tubes thermophoresis will contribute significantly to the total amount of ash deposition. Fig (8-a). illustrate, the second row of the tube has the lowest deposition. As shown in fig(8-b) the fourth row of the tube has the lowest deposition

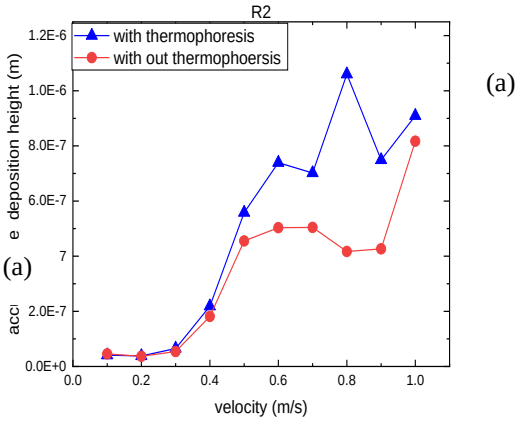

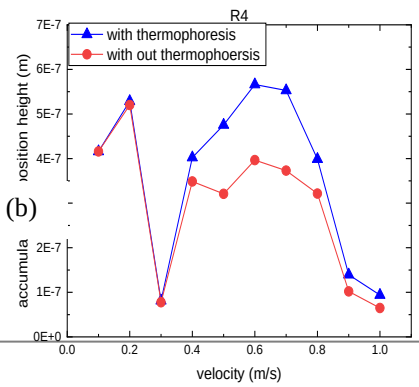

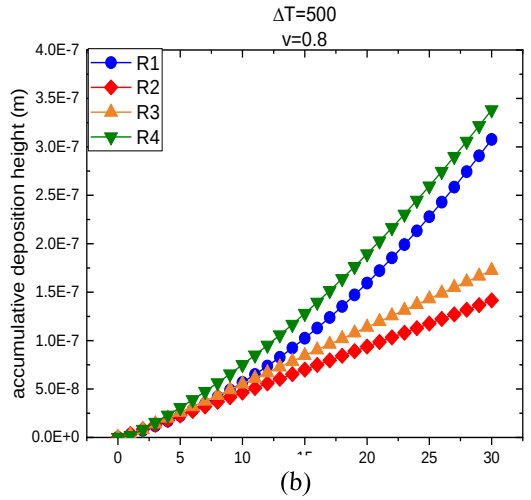

(b)

Fig .8 Effects of temperature gradient on the accumulative deposition height

3.4 Effects change inlet flue gas velocity on the deposition height.

This study the change inlet flue gas velocity on the deposition height through 30 second. Fig (9) Deposition height of bundle tube as the function of time (comparing the different ΔT with constant velocity) Fig (9), illustrates the deposition height the comparing the constant temperature difference between the inlet flue gas and the surface tube =500K, and varying velocity =0.4, v=0.8. As shown in fig(9-a) (9-b) the second row of the tube have the lowest deposition. Furthermore, there is an obvious first row of tube higher deposition presented in fig (9-a). while. As shown in fig(9-b), the fourth row of the tube has higher deposition. because increasing velocity.

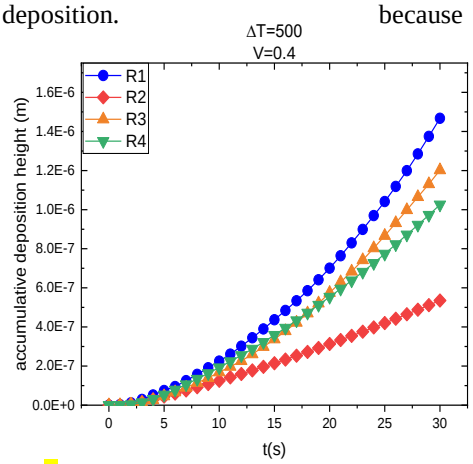

Fig.9 Effects change inlet flue gas velocity on the deposition height

4- Conclusions

In this study, two dimensions' numerical simulations of the ash depositions on the tube bundle are based on the investigation. Programming procedure in CFD by using ANSYS FLUENT 2020R1 has been to simulations that predict the accumulative depositions height on the tube bundle through model discrete phase model (DPM). For the current study, the finite volume method is used to solve governing equations with certain assumptions and appropriate boundary conditions to clarify modelling aims and conditions. This work investigates the ability to use numerical simulations to predict the accumulative ash deposition on the tubes by using the tools DPM and studied the factors that importantly influenced ash deposition with the mechanism's depositions and without. The main conclusions that can be drawn from this current study are as follows:

1. The current work showed that fluent code played an important to predict the accumulative ash depositions, and studied the depositions mechanisms forces (such as thermophoresis forces) that can have influenced ash deposition on the tube bundle with important factors such as (temperature gradient) and (change velocity inlet flue gas)
2. The results show the thermophoresis forces effect significantly on ash with thermophoresis increasing the ash depositions. while without thermophoresis the accumulative deposition height decreases about on the first row (0.12%), seconds row about 0.1%), third row about 0.01%) and four row about (0.12%)
3. The results show that the accumulative ash depositions in the four row increase with time and the front row the accumulative deposition is higher than of the two rows last

Where:
R1: represent to the three pipes in first row
R2: represent to the two pipes in second row
R3: represented to the three pipes in third row
R4: represent to the two pipes in fourth row

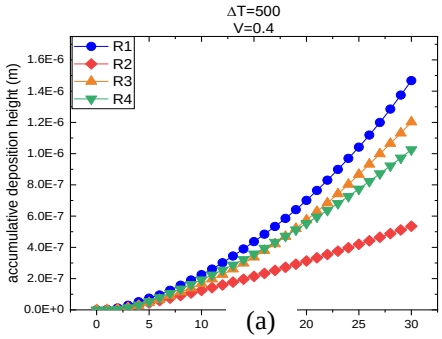

(a)

REFERENCEES

[1] L. L. Baxter and R. W. DeSollar, "A mechanistic description of ash deposition during pulverized coal combustion: predictions compared with observations," *Fuel*, 72, 10,. 1411, 1993,

[2] A. F. Stam, W. R. Livingston, M. F. G. Cremers, and G. Brem, "Review of models and tools for slagging and fouling prediction for biomass co-combustion," *Rev. Artic. IEA*,. 1,. 1, 2010, [Online]Available:http://www.ieabcc.nl/publicatio

ns/slagging_fouling_in_cofiring.pdf.

[3] R. W. Bryers, “Fireside slagging, fouling, and high-temperature corrosion of heat-transfer surface due to impurities in steam-raising fuels,” *Prog. Energy Combust. Sci.*,. 22, 1,. 29, 1996,

[4] J. Tomeczek and H. Palugniok, “Kinetics of mineral matter transformation during coal combustion,” *Fuel*, 81, 10,. 1251, 2002,

[5] T. F. Wall, “Mineral matter transformations and deposition in pulverised coal combustion .,”. 1119, 1992.

[6] P. M. Walsh, A. N. Sayre, D. O. Loehden, L. S. Monroe, J. M. Beér, and A. F. Sarofim, “Deposition of bituminous coal ash on an isolated heat exchanger tube: Effects of coal properties on deposit growth,” *Prog. Energy Combust. Sci.*, . 16, . 4,. 327, 1990,

[7] J. Frandsen, U. Kleinhans, C. Wieland, F. J. Frandsen, and H. Spliethoff, “Ash formation and deposition in coal and biomass fired combustion systems : Progress and challenges in the field of ash particle sticking and rebound behavior Publication date : Publisher ’ s PDF , also known as Version of record Ash formation and deposit,” *Prog. Energy Combust. Sci.*,. 68, 658, 2018,

[8] H. Wang and J. N. Harb, “Modeling of ash deposition in large-scale combustion facilities burning pulverized coal,” *Prog. Energy Combust. Sci.*, 23,. 3,. 267, 1997,

[9] L. Y. Huang, J. S. Norman, M. Pourkashanian, and A. Williams, “Prediction of ash deposition on superheater tubes from pulverized coal combustion,” 1996.

[10] B. E. Lee, C. A. J. Fletcher, S. H. Shin, and S. B. Kwon, “Computational study of fouling deposit due to surface-coated particles in coal-fired power utility boilers,” *Fuel*,. 81,. 15,. 2001, 2002,

[11] Z. Ma *et al.*, “A comprehensive slagging and fouling prediction tool for coal-fired boilers and its validation/application,” *Fuel Process. Technol.*, 88,. 11,. 1035, 2007,

[12] X. Yang, D. Ingham, L. Ma, H. Zhou, and M. Pourkashanian, “Understanding the ash deposition formation in Zhundong lignite combustion through dynamic CFD modelling analysis,” *Fuel*, 194,. 533, 2017,

[13] R. P. Gupta, T. F. Wall, and L. Baxter, “Impact of Mineral Impuritiesin Solid Fuel Combustion,” 2002.

[14] T. Kupka, K. Zając, and R. Weber, “Effect of fuel type and deposition surface temperature on the growth and structure of an ash deposit collected during co-firing of coal with sewage sludge and sawdust,” *Energy and Fuels*, 23,. 7,. 3429, 2009,

[15] J. Li, M. Zhu, Z. Zhang, K. Zhang, G. Shen, and D. Zhang, “Characterisation of ash deposits on a probe at different temperatures during combustion of a Zhundong lignite in a drop tube furnace,” *Fuel Process. Technol.*, 144,. 155, 2016,

[16] C. Luan, C. You, and D. Zhang, “An experimental investigation into the characteristics and deposition mechanism of high-viscosity coal ash,” *Fuel*, 119, 14, 2014,

[17] H. Zhou, B. Zhou, H. Zhang, and L. Li, “Behavior of fouling deposits formed on a probe with different surface temperatures,” *Energy and Fuels*, 28,. 12,. 7701, 2014,.

[18] S. Balakrishnan, R. Nagarajan, and K. Karthick, “Mechanistic modeling, numerical simulation and validation of slag-layer growth in a coal-fired boiler,” *Energy*,. 81, 462, 2015,

[19] R. Weber, M. Mancini, N. Schaffel-Mancini, and T. Kupka, “On predicting the ash behaviour using Computational Fluid Dynamics,” *Fuel Process. Technol.*, 105, 113, 2013,

[20] H. Zhou, P. A. Jensen, and F. J. Frandsen, “Dynamic mechanistic model of superheater deposit growth and shedding in a biomass fired grate boiler,” *Fuel*, 86, 10. 1519, 2007,

[21] H. Zhou, K. Zhang, Y. Li, J. Zhang, and M. Zhou, “Simulation of ash deposition in different furnace temperature with a 2D dynamic mesh model,” *J. Energy Inst* 92, 6,. 1743, 2019,

[22] J. Katz, *Introduction to Computational Fluid Dynamics*. 2012.

[23] “ANSYS Fluent Theory Guide,” no. January, 2020.

[24] B. Zhao, Y. Zhang, X. Li, X. Yang, and D. Huang, “Comparison of indoor aerosol particle concentration and deposition in different ventilated rooms by numerical method,” *Build. Environ.*, 39, 1, 1, 2004,

[25] H. Lu, L. Lu, and Y. Jiang, “Numerical study of monodispersed particle deposition rates in variable-section ducts with different expanding or contracting ratios,” *Appl. Therm. Eng.*, 110, 150 161, 2017, 10.1016/j.applthermaleng.2016.08.167.

[26] Z. Xu, Z. Han, A. Sun, and X. Yu, “Numerical study of particulate fouling characteristics in a rectangular heat exchange channel,” *Appl. Therm. Eng.*, 154, January, 657, 2019,

[27] M. C. Paz, J. Porteiro, A. Eirís, and E. Suárez, “Computational model for particle deposition in turbulent gas flows for CFD codes,” *WIT Trans. Eng. Sci.*,. 68,. 135, 2010, [28] D. R. Willis, “N a Heated Boundary Layer,” *Mech. Eng.*, 1980.

[29] A. Li and G. Ahmadi, “Dispersion and deposition of spherical particles from point sources in a

turbulent channel flow," *Aerosol Sci. Technol.*, vol. 16, no. 4, pp. 209–226, 1992, [30]P. G. Saffman, "The lift on a small sphere in a slow shear flow," *J. Fluid Mech.*, 22,. 2,. 385, 1965,

[31] S. Kalisz, "using Fluent code ot predict deposition during combustion of solid," *J. Inst. Energy*,. 2011, 294, 2011.